Confidential Information: Revised manuscript re-submitted to FEMS Microbiology Ecology

Biogeochemical gold cycling selects metal-resistant bacteria that promote gold particle transformation

Santonu Kumar Sanyal [a,b], Jeremiah Shuster [a,b]#, Frank Reith [a,b]

[a] The University of Adelaide, School of Biological Sciences, Department of Molecular & Biomedical Science, Adelaide, South Australia, Australia

[b] CSIRO Land and Water, Environmental Contaminant Mitigation and Technologies, PMB2, Glen Osmond, South Australia, Australia

#Address correspondence to Jeremiah Shuster, jeremiah.shuster@adelaide.edu.au

Running Title: Bacterial diversity during gold biogeochemical cycling

Abstract

Bacteria catalyze the dissolution and re-precipitation of gold, thereby driving the biogeochemical cycle of gold. Dissolution of gold/silver and re-precipitation of gold transforms gold particles by increasing gold purity. While soluble gold complexes are highly cytotoxic, little is known about how gold cycling affects bacterial communities residing on gold particles. Micro-analysis of gold particles obtained from Western Australia revealed porous textures and aggregates of pure gold nanoparticles, attributable to gold dissolution and re-precipitation, respectively. By interpreting structure and chemistry of particles, the kinetics of gold biogeochemical cycling at the site was estimated to be 1.40×10^{-9} M $year^{-1}$. Bacterial communities residing on particles were composed of Proteobacteria (42.5%), Bacteroidetes (20.1%), Acidobacteria (19.1%), Firmicutes (8.2%), Actinobacteria (3.7%), and Verrucomicrobia (3.6%). A bacterial enrichment culture obtained from particles

contained a similar composition. Exposure of enrichments to increasing concentrations of soluble gold decreased community diversity and selected for metal-resistant bacteria. Lower gold concentrations, which corresponded well with the concentration from the kinetic rate, provided a selective pressure for the selection of metal-resistant organisms while retaining the overall diversity. In conclusion, biogeochemical gold cycling directly influences bacterial communities on gold particles, thereby contributing to a continuum of particle transformation.

Keywords: Bacteria, Biofilms, Gold, Geomicrobiology, Placer, Bio-mineralisation,

Introduction

In natural and engineered environments, biogeochemical cycling of gold and silver acts upon gold particles and transforms them by increasing gold purity over time (*e.g*., Reith et al. 2007). This is initiated through gold and silver dissolution and is completed by reductive gold re-precipitation leading to the formation of pure secondary gold. These processes can occur simultaneously on gold particles and are catalyzed by bacteria occurring on the gold particles (see reviews by Reith et al. 2007; Southam *et al*. 2009; Shuster and Reith 2018; Sanyal, Shuster and Reith 2019 and references therein). The challenge with studying biogeochemical gold cycling within natural systems is that the conditions promoting gold dissolution are highly variable and making gold dissolution processes a rate limiting steps in the cycle. In contrast, gold re-precipitation occurs rapidly as various organic (*i.e*., cells/biofilms, humic substances, extracellular polymeric substances (EPS)) and inorganic *(i.e*., clays, iron oxide minerals) substances can act as a reductants for soluble gold (Karthikeyan and Beveridge 2002; Cohen and Waite 2004); Lengke *et al*. 2006; Zhu *et al*. 2009; Kenney *et al*. 2012, Song, Jang and Kim 2012).

From a materials approach, these processes have been interpreted through the characterisation of secondary gold structures (*e.g*., nanoparticles and microcrystals) occurring on placer gold, and comparing these structures to biomineralized gold formed *in-vitro* through the reductive precipitation and biomineralisation of soluble Au(I/III)-complexes by various types of bacteria (Southam and Beveridge 1994; Lengke *et al*. 2006; Lengke and Southam 2007; Fairbrother *et al*. 2013; Shuster *et al*. 2014; Shuster *et al*. 2015). In doing so, polymorphic layers on gold particles (*i.e*., regions containing bacteria, clays, secondary gold structures on particles) have been identified as likely "hot spots" for gold dissolution and re-precipitation to occur (Reith *et al*. 2006; Reith *et al*. 2009; Reith *et al*. 2012). By characterizing gold nanoparticles associated within clays, temporal estimates suggested that biogeochemical gold cycling linked to significant transformation of placer particles within sub-tropical environments can occur on decadal time scales (Shuster *et al*. 2017). However, a kinetic (or turnover) rate for gold biogeochemical cycling taking into account secondary gold concentrations within gold-bearing soil from a weathering environment have not been estimated to date. The development of such a "kinetic" model for gold turnover is important, because knowing rates of gold dispersion within the weathering environment can aid gold exploration with the discovery of new deposits.

From a microbiological perspective, studies delineating gold dissolution and re-precipitation processes have characterized bacterial communities existing on the surface of gold particles from tropic to sub-arctic environments (Reith *et al*. 2018 and references therein). A common trend among particles is that phylogenetically diverse bacterial communities exist within polymorphic layers. Interestingly, a negative correlation exists between the diversity of bacterial communities on particles and the degree of particle

transformation (Rea *et al*. 2018; Rea *et al*. 2019). In addition, it has been suggested that soluble gold produced during gold particle dissolution could provide a selective pressure for the enrichment of metallophilic microbes on particles (Rea *et al*. 2018). However, there is no empirical evidence for this selective process, because the bacterial community identified on a particle only represents a “snap shot” of its diversity at that time of sampling and does not capture how it changes or develops over time. Specific biochemical functions to deal with gold toxicity and detoxify soluble gold have developed in key-species living on the particles such as *Cupriavidus* metallidurans and *Delftia acidovorans* (Reith *et al*. 2009; Johnston *et al*. 2013; Wiesemann *et al*. 2017; Bütof *et al*. 2018). Understanding the development of biofilm communities on gold particles may aid ore processing and the recovery of gold from waste materials (*e.g.*, electronic waste) in the future. Therefore, the aims of this study are to: i) estimate the turnover rate of gold during biogeochemical cycling; ii) determine how mobile gold affects bacterial communities derived from the surface of particles *in-vitro*; and iii) identify links between these factors, which could contribute to the observed transformation of particles. We hypothesize that the development of metal-resistant bacterial communities on gold particles is primarily dependent upon the biogeochemical cycling of gold to provide soluble gold a selective pressure. As a result, these metal-resistant bacteria can form functional biofilms, thereby perpetuating gold dissolution and a continuum of the gold biogeochemical cycle (*i.e*., a positive feedback loop). To test this hypothesis, a multi-analytical approach was used to study the chemistry and structure of gold particles and bacterial communities residing on particle surface. Therefore, this study highlights the importance of interdisciplinary studies to gain a holistic understanding of biogeochemical processes occurring in natural and engineered environments.

Materials and Methods

Site description and sample acquisition

The sampling site is located near the town of Donnybrook (33.58°S 115.82°E), which is approximately 200 km south of Perth, Western Australia. This site is situated in a region that was once important for mining due to an accessible gold-bearing epithermal deposit (Geological Survey of Western Australia 1998). Geologically, the site is situated east of the Darling fault and underlain by Archaean granitic rocks that have been subjected to mechanical erosion by an ancient river system, which formed the Donnybrook sandstone sequence (Geological Survey of Western Australia 1998). Climate at the site is warm-temperate, with an average annual temperature of 22.6 °C and average annual rainfall of 972.5 L m^{-2} (Bureau of Meteorology, Australia; http://www.bom.gov.au). Seventy to eighty percent of annual rainfall occurs during the winter months (*i.e*., May to September), which leads to either waterlogging or extensive erosion of soils. In contrast, the summer months tend to be hot and dry (Bennett and Richard 2002; Bureau of Meteorology, Australia; http://www.bom.gov.au). These climatic conditions support the re-establishment of native flora on mullock heaps since mining activity ceased. During a field expedition in October 2016, *Eucalyptus* sp*.* and *Allocasuarina* sp*.* trees as well as a variety of sparse low shrubs and grasses such as *Acacia* sp. and *Austrodanthonia* sp. were observed.

Gold was first discovered in 1897 and underground mining, which involved digging shafts through sandstone and mudstone, persisted for three decades (Freeman and Donaldson 2004; Backhouse and Wilson 1989). During gold extraction, the waste rock was discarded into piles commonly referred to as “mullock heaps”. By the early 1930s, industrial-scale mining activity ceased due to increasing paucity in gold recovery and the mines and

mullock heaps were abandoned. Today, local knowledge from artisanal miners and gold-prospecting hobbyist ascertained the presence of residual gold within mullock heaps, which is attributed to the inefficacies of historic extraction. As these mullock heaps and the gold particles have been subjected to biogeochemical weathering for a geologically short but well defined number of years (*i.e.*, 86 years since the last mining activity), the site is an ideal location for estimating the turnover rates of gold biogeochemical cycling. In turn, the effect of gold biogeochemical cycling on bacteria occurring on the surface of gold particles can also be studied. Therefore, 100 kg of soil was collected from an equivalent 1 m^2 plot with a maximum depth of 30 cm on a mullock heap. A 500 g aliquot was sifted (described below) and saved for geochemical analysis. The remaining soil was sluiced and panned using the field-sterile procedures for gold particle acquisition outlined by Reith *et al*. (2010). A total of 60 gold particles were obtained and used for micro-analytical and microbiological analyses.

Scanning electron microscopy and electron microprobe analysis of gold particles

At the time of sampling, 20 gold particles were immediately placed in Eppendorf tubes containing a fixative solution (*i.e.*, 4 wt.% paraformaldehyde, 1.25 wt.% glutaraldehyde, 4 wt.% sucrose in phosphate-buffered-saline solution adjusted to pH 7.2). The purpose for fixation is to preserve the structure of any microbes or biofilms occurring on the surface of the gold particles. The gold particles were dehydrated using a serial 2 × 70 $wt.\%_{(aq)}$, 90 $wt.\%_{(aq)}$, and 3 × 100 $wt.\%_{(aq)}$ ethanol with 10 min incubations for each concentration. The particles were then placed in a 1:1 mixture of 100 wt.% hexamethyldisilazane (HMDS) with 100 wt.% ethanol and incubated for an additional 10 minutes. This last step was repeated before placing the particles into 100 wt.% HMDS and incubated for an additional 30 minutes. After incubation, the HMDS was removed and discarded and the particles were allowed to

air-dry. Once dry, the gold particles were placed on aluminum stubs using carbon adhesive tabs and coated with a 10 nm thick deposition of carbon. Particles were characterized using a FEI Quanta 450 Scanning Electron Microscope (SEM) and a FEI Helios Nano-Lab Dual Beam Focused Ion Beam (FIB) SEM equipped with Energy Dispersive Spectrometers (EDS). Secondary electron (SE) and backscatter electron (BSE) micrographs were obtained using 5 kV and 20 kV, respectively. Selected gold particles were FIB-milled to obtain high-precision cross-sections at the particles' surface. Milling was performed using 20 kV and 9.7 pA electron current.

Scanning electron microscopy analysis was used to select six representative particles for electron microprobe (EMP) analysis. The selected particles were embedded in epoxy-resin and polished to obtain cross-sections through the particle. The polished samples were analyzed using a Cameca™ SX100 microprobe equipped with five wavelength dispersive (WLD) X-Ray detectors, operating at 20 kV and 200 nA. The EMP software (CalcImage) generated a full quantitative pixel-by-pixel calculation using a mean atomic number background correction. The corrected EMP data was analyzed in Surfer10™ to produce net intensity maps of the polished gold particles. The detection limit for gold and silver was 0.24 wt.% and 0.09 wt.%, respectively. Both elements were calibrated to pure metal stands purchased from Astimex and P&H.

Geochemical analyses of the gold-bearing sediment

At the time of sampling, visible gold particles were removed from the 500 g soil aliquot, so that only invisible nano- and micro-phase secondary gold adsorbed to soil materials remained. Once free of visible gold, the soil was pulverized according to the method described by Reith *et al.* (2018) to homogenize the sample prior to microwave

digestion in concentrated *aqua regia*. The elemental composition of the soil was determined using an Agilent 7700 inductively coupled plasma-mass spectrometer (ICP-MS) calibrated with National Institute of Standards and Technology's (NIST) standards. Detection limits (mg kg^{-1}) for each element were: Na (40), Mg (100), Al (100), P (100), S (40), K (100), Ca (100), V (0.1), Mn (20), Fe (100), Co (0.2), Cu (0.2), Zn (0.2), As (0.1), Se (0.2), Mo (0.1), Ag (0.1), Cd (0.1), Sn (0.1), Au (0.1), Pb (0.1), U (0.1).

Estimating the kinetics of gold by biogeochemical cycling

To estimate the turnover rates of gold at the site, gold intensity EMP maps, which represent a 'slice' through a particle, were used. The area of each slice was calculated by analyzing EMP maps using ImageJ software. In doing so, the number of pixels representing the particle was divided by the known dimensions of one pixel. Similarly, the number of pixels representing pure secondary gold were counted and area was calculated. The EMP analysis had an average sampling depth of 0.2 µm; therefore, the area of each gold particle slice as well as secondary gold was converted to volume. Particle volume was estimated by using the average mass of 20 particles (4.25×10^{-4} g), measured weight percent (*i.e.*, based on EMP analysis), and densities of gold and silver (*i.e.*, 19.32 g cm^{-1} and 10.5 g cm^{-1}, respectively). Using the average moles of secondary gold per particle, the moles of gold for 60 particles (*i.e*., the number of particles in 100 kg of soil) was determined. To obtain the total moles of secondary gold in 100 kg of soil, the amount of dispersed ultrafine and adsorbed secondary gold detected in the soil by ICP-MS was added to the moles of secondary gold on the 60 particles. With this variable along with the minimum length of time *in-situ* (*i.e*., 86 years), and the average annual rainfall for this region (*i.e*., 972.5 L m^{-2};

Australian BOM http://www.bom.gov.au), the kinetics of gold biogeochemical cycling within the mullock heaps was estimated. See Table 1 for detailed descriptions of calculations.

Bacterial diversity profiling of gold particles

A total of 15 gold particles were repeatedly washed with sterile 0.9% NaCl solution to remove any residual sediment and placed in sterile, PCR-tubes containing fresh 0.9% NaCl solution. A two-step nested polymerase chain reaction (PCR) of direct amplification from gold particles and targeting a portion of 16S rRNA gene was performed. It is important to note that this direct PCR method was extensively tested in previous studies and subsequently used to study bacteria occurring on individual gold particles (*e.g*., Reith *et al*. 2006; Reith *et al*. 2010; Rea *et al*. 2018; Reith *et al*. 2018). For the initial PCR amplification, universal primers 27F and 1492R were used and positive amplicons were further amplified using primers 27F and 519R (Reith *et al*. 2018). Amplification of DNA was performed in a Thermal Cycler (Applied Biosystems Veriti™). To test for PCR contamination, negative controls from the first round were used as template for the second round of PCR, only when first and second round negative controls were clean samples were used for NGS. All 15 gold particles were PCR-positive; 5 PCR-positive gold particle amplicons were kept as a reserve. High-throughput sequencing was performed using the Illumina MiSEQ platform – TruSeq SBS v.3 targeting 300 bp pair sequence of 10 PCR positive gold particle amplicons following the methods established by Bissett *et al*. (2016). See Supplementary Information for detailed methods regarding PCR and sequencing procedures and Table S1 for primers.

Enrichment cultures from gold particles

Selective enrichments were amended with soluble gold (*i.e*., Au(III)-chloride) to assess how bacterial diversities and abundances may change when particles undergo dissolution during gold biogeochemical cycling. Gold concentrations used for the enrichment were within the range of gold concentrations occurring in soils and micro-zones around gold particles (McHugh 1988; Benedetti and Boulëgue 1991; Ta *et al*. 2014). For the enrichment of a bacterial consortia from the particles a total of 20 gold particles were directly inoculated into a sterile centrifuge tube containing 20 mL of TRIS Minimal Medium (TMM) containing sodium gluconate as a carbon-source (Mergeay *et al*. 1985). These enrichments were placed in a 25˚C rotary shaker or 14 days. After incubation, a 5 mL aliquot of this primary enrichment was kept for DNA analyses. Using sterile conical flasks, a 1 mL aliquot of the primary enrichment was transferred to 50 mL of fresh TMM. This served as a control that was performed in parallel with a 1 mL aliquot of primary enrichment that was transferred to 50 mL TMM containing 0.01 µM Au. Secondary, tertiary and quaternary enrichments were transferred to fresh media containing 0.1, 1, and 10 µM Au, respectively, to understand how bacterial diversities change under increasing gold stress. All enrichments were incubated for 5 days at 25˚C in a rotary shaker in the dark to prevent any photocatalytic effects. After incubation, 5 mL aliquots from each enrichment were used for DNA extraction using a PureLink™ Microbiome DNA Purification Kit (Thermo Fisher Scientific, Australia). Extracted DNA was subjected to PCR amplification targeting 16S rRNA gene and next-generation sequencing (NGS) was performed using the Illumina MiSEQ platform (TruSeq SBS v.3) using 300 bp paired-end sequencing as described above.

Bioinformatics and multivariate statistical analysis

For data from either culture-independent or culture-dependent experiments, bioinformatic analysis of the sequences was performed following the methods established by Bissett *et al*. (2016). Briefly, the sequence read quality was evaluated using FastQC (Andrews 2010). Sequences were trimmed to low-quality bases and merged using FLASH (Magoč and Salzberg 2011). Sequences <400 bp, containing unidentified bases (N) or homopolymers runs of >8 bp, were removed using MOTHUR (v1.34.1). Remaining sequences were then analyzed using UPARSE for simultaneous chimera filtering and OTU clustering (OTUs of ≥ 97 % similarity). An OTU abundance table was constructed by mapping all reads to the OTUs using usearch_global. Taxonomic classification of OTUs (to genus level) were carried out using MOTHUR's implementation of the Wang classifier. Taxonomic identification of the OTUs were performed using the Greengenes database (http://greengenes.lbl.gov). Additionally, the partial 16S rRNA gene sequences of OTUs were subjected to BLASTN analysis (http://www.ncbi.nlm.nih.gov/) for more accurate species level identification based on showing significant homology. Multivariate statistical analyses were conducted using the PRIMER-6 software with add-on PERMANOVA+ (Clarke *et al*. 2014; Anderson and Gorley 2007). Similarity matrices were generated on square-root-transformed sequence abundance data from the culture-independent experiment using the Bray-Curtis method (Bray and Curtis 1957). Similarities between communities on individual particles were assess using hierarchical cluster analysis (similarity profile analysis or SIMPROF, $P < 0.05$).

Sequences from the culture-independent and culture-dependent experiments were deposited in GenBank with the accession numbers MH698582-MH698623 and MH706982-

MH707020, respectively. Sequences were used to construct cladograms using MEGA version 4.0 and applying the maximum-likelihood (1000 bootstrap replicates) statistic parameter (Tamura *et al*.2007) and further analyzed using the Interactive Tree of Life (https://itol.embl.de/) online platform. Using the cladogram of the culture-independent experiment, bacteria were group into four putative biochemical functional groups; these are carbon- and nitrogen fixation, biofilm development including EPS production and auto-aggregation, as well as gold biotransformation. Categories were chosen based on the extensive cataloging of putative biochemical functions of bacteria occurring on gold particles (see Rea *et al*. 2016 and reference therein; Besemer *et al*. 2012; Levipan and Avendano-Herrera 2017). To assess the changes in bacterial abundance and diversity in the enrichment culture experiments, three groups describing different exposures were used: no gold (*i.e*., subculturing of the primary enrichment), low gold concentrations (*i.e*., enrichments exposed to 0.01 and 0.1 µM Au, respectively), and high gold concentrations (*i.e*., enrichments exposed to 1 and 10 µM Au, respectively). Differences between grouped treatments were assessed using the pairwise t-testing within PERMANOVA routine, with partial sums of squares on 9,999 permutations on an unrestricted permutation of raw data model.

Results

Gold particles and host sediment characterisation

Gold particles were dendritic with overall fern-leaf like morphologies and ranged between 0.2 to 3.2 mm along the longest measurable length (Fig. 1A). Scanning electron microscopy revealed that the surfaces of the particles were rough and contained polymorphic layers comprised of abundant secondary gold, EPS, clay minerals and

microbial cells. Secondary gold occurred as nanoparticles and aggregates in the form of either pseudo-spheres or euhedral crystals (Fig. 1B, C). Dissolution features occurred as micrometer-scale pores, which gave particles a spongy surface texture (Fig. 2A). Nanoparticulate gold aggregates often occur in close proximity to these dissolution features (Fig. 2A). Focused ion beam-milled cross-sections demonstrated that porous dissolution features continue beneath the outer surface of the particles (Fig 2B). Pore spaces deeper within the particle were nanometer in size, whereas pores directly beneath aggregated nanoparticles were micrometer in size and contained EPS (Fig. 2B and inset). Energy dispersive spectroscopy identified gold and silver variations from these structures: consolidated regions contain 62.4 to 69.0 wt.% gold (Fig. 2C, spots 1–6, 11–13, 16–17), porous regions contain 77.7 to 98.0 wt.% gold (Fig. 2C, spots 7–10, 14, 15, and 18), secondary aggregates contain ≥99.0 wt.% gold (Fig. 2C, spots 19–23). This was confirmed using electron microprobe analysis, which showed that the distribution of gold and silver within the particles is heterogeneous. While the cores of particles are composed of a gold-silver alloy with an average composition of 68.3 wt.% gold and 31.7 wt.% silver, outer sections of the particles are often composed of pure (≥ 99.0 wt.%) secondary gold (Fig. 2D). The concentration of secondary gold dispersed within the soil was 0.23 mg kg^{-1}, which is equivalent to 1.17×10^{-4} moles secondary gold in 100 kg of soil. In contrast, silver was not detected. See Table S2 for full elemental composition of soil.

Kinetics of gold turnover

The presence of secondary gold enriched on visible gold particle surfaces as well as dispersed in the soil strongly suggests that gold has been subject to biogeochemical cycling. Mass balance calculations show that primary and secondary gold contained in the 60

collected particles accounted for 47.5 % of gold in the system (*i.e*., the 100 kg of soil); with primary gold from gold-silver alloys accounting for 36.0 % and secondary pure gold accounting for 11.5 % of all gold. This means that the majority of gold in the system (*i.e.*, 52.5 %) was dispersed within the soil. In turn, this also means that more than 60 % of all gold in the system has likely been the subjected to biogeochemical cycling in the last 86 years. Within the mullock heap, the mass balances in combination with calculations explained above and shown in Table 1, estimate the turnover of gold by biogeochemical cycling to be 1.40×10^{-9} M $year^{-1}$.

Community composition of biofilms residing on gold particles

High-throughput sequencing of PCR-positive amplicons produced a total of 978.000 high-quality sequence reads. Bacterial communities on individual particles were diverse and comprised between 26 and 41 different operational taxonomic units (OTUs). Cluster analyses revealed similarities of 44 to 75 % between bacterial communities derived from different particles, with similarity profile analysis (SIMPROF, $P < 0.05$) showing that only two significantly different groups of particles associated communities existed (Fig. 3A). These were combined to constitute a representative bacterial community of 46 OTUs that is representative of the community residing on gold particles from the Donnybrook site. It contained: Alpha-proteobacteria (16.7 %), Beta-proteobacteria (9.8 %), Gamma-proteobacteria (14.9 %), Delta-proteobacteria (1.0 %), Bacteroidetes (20.1 %), Acidobacteria (19.1 %), Firmicutes (8.2 %), Actinobacteria (3.7 %), Verrucomicrobia (3.6 %), and 2.9 % of reads that were unclassified bacteria (Fig. 3B). Twenty-five of these OTUs were further classified following Rea *et al*. (2016) as microorganisms putatively capable of carbon- or nitrogen fixation, biofilm development, and gold biotransformation. Of these, Bacteroidetes

constituted the largest group (11 OTUs), of which five were attributed to biofilm development (*i.e*., *Flavobacterium* sp. (OTU 10), *Arcicella* sp. (OTU 4), *Sphigobacterium* sp. (OTU 31), *Porphyromonas* sp. (OTU 35), and *Sediminibacterium* sp. (OTU 36)) (Fig. 4). The classified Alpha-proteobacteria (7 OTUs) contain putative carbon and nitrogen fixers and biofilm developers (2 OTUs each), and gold bio-transformers (1 OTU). Beta-proteobacteria and Gamma-proteobacteria each constituted 6 and 5 OTUs, respectively, which were associated with either biofilm development (1 and 3 OTUs respectively) or gold biotransformation (2 and 4 OTUs, respectively) (Fig. 4). Actinobacteria contained 6 OTUs, three of which were attributed to gold biotransformation (Fig. 4). Specifically, the OTUs for gold biotransformation included metallophilic microbes such as *Cupriavidus* sp. (OTU 45), *Burkholderia* sp. (OTU 39), *Arthrobacter* sp. (OTU 17), *Shewanella sp.* (OTU 3), *Stenotrophomonas* sp. (OTU 23), *Sphingomonas* sp. (OTU 24), and *Serratia sp*. (OTU 11). The remaining OTUs (23) could not be classified with respect to the four putative biochemical functions.

Bacterial diversity profiling in selective enrichment experiments

A primary enrichment culture was obtained from 20 gold particles. Next generation sequencing confirmed that this consortia contained 39 distinct bacterial OTUs belonging to Alpha-proteobacteria, Beta-proteobacteria, Gamma-proteobacteria, Bacteroidetes, Acidobacteria, Actinobacteria (Fig. 5). Overall, this initially enriched community was similar to the community detected on the gold particles using direct PCR (Figs. 4 and 5). In general, bacterial diversity across all phyla decreased with exposures to increasing concentrations of soluble gold, while metal resistant microbes were selected (Fig. 5 to 7). When the initial enrichment was exposed to 0.01 µM Au, 67 % of the original OTUs were retained. With subsequent exposures to 0.1, 1.0, or 10 µM Au, 89, 74, and 65 % of the OTUs of the

previous selective enrichment was retained, respectively (Fig. 6 and 7). All phyla within the bacterial community were retained up to the exposure to 0.1 µM Au (Fig. 6); however, the entire Bacteroidetes phylum was eliminated when the enrichment culture was exposed to 1 µM Au (Fig. 7). Within selective enrichments exposed to 1 or 10 µM Au, species belonging to the Proteobacteria (*i.e*., *Pseudomonas* spp., *Cupriavidus* sp., *Stenotrophomonas* sp., *Serratia* sp., and *Sphingomonas* sp.) were retained. Interestingly, these organisms were also detected on gold particles from the culture independent study (Fig. 3). Statistical analysis (*i.e*., t-testing) was used to assess changes in community composition between enrichments subjected to low and high gold concentrations and the community in control incubations not exposed to soluble gold. Results showed that significant changes occurred in enrichment amended with both low gold concentrations ($t = 3.41$, $P < 0.05$) as well as high gold concentrations ($t = 2.43$, $P < 0.05$). It is important to note that differences between the primary enrichment and subculte as well as between the enrichments amended with low and high gold concentrations were not significant.

Discussion

Interpreting gold transformations during biogeochemical cycling

Gold particles from a primary sources are typically composed of gold-silver alloys and are angular in shape. This chemical composition and morphology reflects the geochemical conditions in which gold was emplaced and mineralised within the host rock (Webster and Mann 1984; Townley *et al*. 2003; Hough, Butt and Fischer-Bühner 2009). Such particles are usually highly irregular in shape and show no signs of rounding, pitting or abrasion, which are commonly observed when particles have been physically transported in Earth's surface environments (Townley *et al*. 2003). In contrast, gold particles occurring in placer deposits

(*e.g*., in colluvial, alluvial or glacial placers) typically exhibit rounded morphologies, often show signs of bending and folding as well as scratched, pitted or gouged surfaces resulting from mechanical reshaping during transport (Townley *et al*. 2003). With respect to the gold particles collected at the Donnybrook site, the overall composition of their cores (*i.e*., 68.3 wt.% gold and 31.7 wt.% silver) as well as the dendritic morphologies (Fig. 1) highlight their primary origin. More importantly, they suggest that little to no mechanical reshaping had occurred since their placement in the mullock heaps.

Gold particles from Earth's surface environments often display porous surface textures and secondary gold nanoparticles and microcrystals, which are attributed to (bio)geochemical rather than physical transformation (*e.g.*, Mossman and Dyer 1985; Bowles 1988; Reith and McPhail 2007; Falconer and Craw 2009; Reith *et al.* 2012; Reith *et al*. 2018; Shuster *et al.* 2015; Rea *et al*. 2018). At Donnybrook, the presence of gold and silver dissolution features, which were closely associated with ≥99.0% pure secondary gold structures on particle surfaces, suggests that particles were subject to intense biogeochemical transformation over the past 86 years (Fig. 1 and 2).

In Earth's surface environments, both gold and silver are mobile (Mann 1984). The lack of silver and high levels of gold detected in the soil at the study site (*i.e*., 0.23 mg kg^{-1}) suggest that silver was widely dispersed in the environment, while gold was re-precipitated in closer proximity to the initial source. Within hydrological regimes, silver is generally more reactive and more readily mobilized compared to gold, which contributes to its greater dispersion in the environment (Boyle 1968; Mann 1984; Settimio *et al.* 2014; Shuster *et al.* 2017). Biogeochemical transformations lead to the formation of soluble gold complexes, which are commonly reduced as secondary gold nanoparticles. These nanoparticles often

occur in close proximity to the gold source and lead to an overall gold enrichment in soils overlying deposits (Reith *et al*. 2005). Indeed, gold complexes and nanoparticles are known to readily adsorb onto clay minerals, organic matter and iron/manganese oxides (Baker 1978; Gatellier and Disnar 1989; Wang, Xie and Ye 1995; Gray 1998; Reith and Cornelis, 2017).

The turnover rate of gold by biogeochemical cycling was calculated to be 1.40×10^{-9} M year^{-1}. Given the average moles of gold in a particle (1.47×10^{-6}) and this turnover rate, it is possible that entire particles could be completely transformed into pure secondary gold in little more than 1000 years. In geological terms this is rapid, especially for a noble element that was conventionally considered to be inert. However, similarly high transformation rates of gold were observed in a recent study of gold particles from Kilkivan, a subtropical environment in Australia (Shuster *et al.* 2017). In contrast, the turnover of gold and transformation of particles from sub-arctic environments (i.e., Finland) were two to three orders of magnitude slower, suggesting that climatic factors, such as ambient temperature and water availability are important in determining biogeochemical gold turnover rates (Reith *et al.* 2018). Indeed, temperature and rainfall determine the rates of major element (*e.g.*, the cycling of carbon, nitrogen and sulfur) cycling (Wollast and Mackenzie 1989). Recent research has shown that an interconnected “web” of elemental cycling governs the gold mobility and drives gold cycling (Sanyal, Shuster and Reith 2019). For example, compounds resulting from the cycling of carbon, nitrogen, and sulfur (i.e., nutrient elements) need to be available for bacteria to: form biofilms on gold particle surfaces, excrete gold-complexing ligands, and provide the energy for bacterial gold detoxification (Sanyal, Shuster and Reith 2019). At Donnybrook, seasonal variations of major element cycling and therefore gold

cycling are expected due to seasonal variations in rainfall (*i.e*., 70 to 80 % of rainfall occurs during the winter months). For long-term gold cycling to occur well into the future, average annual rainfall needs to persist to support conditions for successive biofilm development and growth (*e.g.*, nutrient availability, pH, and salinity). Therefore, it is reasonable to suggest that climate change as well as other anthropogenic activities could alter the kinetics of biogeochemical gold cycling.

Bacterial contributions to the biogeochemical cycling of gold

Gold particles are substrates onto which a diverse range of bacteria can attach, form biofilms, and contribute to gold dissolution as well as gold re-precipitation, thereby facilitating the complete biogeochemical cycle of gold (Reith *et al.* 2010; Shuster *et al.* 2015; Rea *et al.* 2018; Reith *et al.* 2018). In the present study, residual organic material and EPS were observed within polymorphic layers and pores of dissolution features (Fig. 1C and 2B), suggesting that biofilms exist or are developing on the surface of these particles. Direct amplification of the 16S rRNA gene from the gold particles confirmed the presence of a diverse range of bacteria occurring on the surface of the particles (Fig. 3). In terms of diversity, communities were similar to previous studies that identified communities on placer particles from various environments (e.g., Reith *et al.* 2018; Rea *et al.* 2018).

Carbon- and nitrogen-fixing bacteria play an important role in providing bioavailable carbon and nitrogen necessary for colonization by other bacteria to form a multispecies biofilm (Sanyal, Shuster and Reith 2019). Based on the categorization of putative biochemical functions, 16 % of bacteria resident on the Donnybrook particles were involved in either carbon- or nitrogen fixation, including *Rhodobacter* sp., *Porphyrobacter* sp., *Brevundimonas* sp., and *Nitrobacter* sp. Of the remaining categorized OTUs, 40 % were

involved with biofilm development; these include Bacteroidetes as well as a range of Proteobacteria. Previous studies reported that the Bacteroidetes *Sphingobacterium* sp. and *Flavobacterium* sp. detected on the particles, have an important role in surface adhesion/biofilm formations (Besemer *et al*. 2012; Levipan and Avendano-Herrera 2017 see also Figure 3, this study). Proteobacteria belonging to the identified EPS-producing, genera *Pseudomonas*, *Acinetobacter*, *Serratia*, and *Burkholderia*, may further contribute to the structural integrity and rigidity of biofilms (Bezawada *et al*. 2013).

Once formed, these biofilms can excrete large amounts of organic substances including low molecular weight organic acids (*e.g*., carboxylic and amino acids) as well as cyanide as metabolic by-products (Beech and Sunner 2004). These substances act as complexing ligands enabling the dissolution of gold and silver (Korobushkina, Mineev and Praded 1976, Korobushkina, Karavaiko and Korobushkin 1983; Smith and Hunt 1985; Fairbrother *et al.* 2009; and references therein). This provides a starting point for gold biogeochemical cycling and a mechanistic explanation for the existence of dissolution features with EPS on the surface of the gold particles (Fig. 2B, arrow 1). Gold particle dissolution can produce soluble gold complexes that are highly cytotoxic (Wiesemann *et al*. 2013; Wiesemann *et al*. 2018). However, metal-resistant bacteria (*e.g*., *Cupriavidus* sp.) with putative gold transforming functions comprised 44 % of the categorized OTUs. These bacteria ameliorate the toxic effects of gold complexes by actively forming nanoparticles to prevent oxidative and heavy metal stress and avoid cell death (Karthikeyan and Beveridge 2002; Reith *et al.* 2009; Johnston *et al.* 2013; Shuster *et al.* 2015; Bütof *et al*. 2018). Additionally, biomass including cells and EPS are a source of electrons for the reduction of soluble gold complexes, which form pure gold nanoparticles with committal cells death or

EPS degradation (*i.e*., passive biomineralisation, Shuster and Reith 2018 and reference therein). It is important to note that these processes can occur contemporaneously. More importantly, these processes can be perceived as opposing yet complimentary in the context of a cycling; therefore, reduction of soluble gold complexes and the formation of gold nanoparticles “completes” the biogeochemical cycle of golds (Fig. 2B, arrow 3).

The effect of biogeochemical cycling of gold on bacterial communities

Previous studies have shown that heavy metals are an important factor influencing the diversity and function of soil microbial communities (Wakelin *et al.* 2012a; Wakelin *et al.* 2012b). For instance, elevated concentrations of copper, lead, zinc, or cadmium in anthropogenically-polluted soils and sediments have been shown to strongly influence the composition and activity of resident bacterial communities (*e.g*., Bååth 1989; Kizilkaya *et al.* 2004; Abaye *et al.* 2005; Wakelin *et al*. 2012a; Wakelin *et al*. 2012b; Macdonald *et al.* 2011). From microcosm experiments, Reith and McPhail (2006) demonstrated that indigenous soil bacteria were capable of dissolving elemental gold (*i.e.*, an equivalent 1.8 µM Au within 20 to 45 days of incubation) and highlighted the possible effects of soluble gold on microorganisms residing on gold particles. In the present study, the culture-dependent experiments served as a laboratory model of how bacterial diversity of biofilms on gold particles could change during particle transformation, specifically during gold particle dissolution. The lower gold concentrations used in this study (*i.e*., 0.01 and 0.1 µM Au) are considered to be elevated concentrations (Benedetti and Boulëgue, 1991), but were comparable to that which was detected in the Donnybrook soil as well as other Australian gold-bearing soils (Reith and McPhail 2006; Reith and McPhail 2007). The higher gold concentrations used for the tertiary and quaternary enrichments (*i.e.*, 1 and 10 µM Au) can

be considered highly anomalous (Benedetti and Boulëgue, 1991). However, it is possible that these concentrations could exist in localised micro-environments surrounding particles or occur if rates of gold (bio)geochemical cycling increased due to greater rainfall or anthropogenic influences.

In a study by Reith et al. (2012), the exposure of bulk soil microbes to 5 µM Au led to a significant reduction of the overall number of bacterial taxa; exposures to 0.5 mM Au led to an almost complete destruction of the bacterial community due to the strong bactericidal properties of the soluble Au(III) complex (Reith *et al.* 2012). Further analysis of the functional potential of these microbial communities (*i.e.*, GeoChip microarrays) showed an increasing abundance and diversity of metal-resistance genes. In particular, the metal-resistance genes *copA*, *chrA* and *czcA* of the aurophillic bacterium *Cupriavidus metallidurans* CH34, which only occurred in soils overlying gold mineralised regions (Reith *et al.* 2012). From the Donnybrook gold particles, the bacterial diversity of the primary enrichment was comparable to that which was determined by direct amplification (Figs. 3-5); furthermore, the community composition was stable when the primary enrichment was sub-cultured. Therefore, it is reasonable to suggest that the primary enrichment could represent a bacterial community constituting a biofilm on particles. The primary and secondary amended with 0.01 or 0.1 µM Au, respectively, led to the largest statistical changes ($t = 3.41$, $P > 0.05$). While all phyla were still present, a reduction in community diversity was observed (Fig 4 and 5) and these low gold concentrations were sufficient to drive significant community changes. This result was consistent with previous studies involving the exposure of microbial communities from bulk soils, associated with varying degrees of gold mineralization, to soluble gold (Reith and Rogers 2008; Reith *et al*. 2012). More importantly, this result confirmed that bacterial

communities from gold particles are highly sensitive to very low levels of soluble gold. While these concentrations can be cytotoxic, it suggests that functional adaptions may also occur. Respective enrichments amended with 1 and 10 µM Au represented bacterial populations that have been affected by higher gold concentrations. While the community diversity further declined, the most notable change was the complete elimination of Bacteriodetes after the exposure to 1 µM Au. This phylum originally constituted 20.1% of bacterial community on gold particles. Bacteriodetes are known to contribute to surface conditioning and EPS formation for biofilm development, but are commonly not known to be highly resistant to heavy metals (Lo Giudice *et al*. 2013; Ding *et al.* 2015; Beech and Sunner 2004; Harrison *et al.* 2007). Conversely, metal-resistant bacteria such as *Cupriavidus* sp., *Pseudomonas* sp., *Stenotrophomonas* sp., *Serratia* sp., and *Sphingomonas* sp. were selected in enrichments exposed to higher gold concentrations and were also consistent with studies involving the enrichment of gold-tolerant (Rea *et al*. 2016; Reith *et al*. 2018). Therefore, selection of metal-resistant bacteria from Donnybrook particles supports the notion that the retention of these bacteria would perpetuate biogeochemical gold cycling and particle transformation by a multispecies biofilm with diverse biochemical functions (Fig. 8).

Conclusions

In this study, a diverse bacterial community residing on gold particles from mullock heaps in Donnybrook, Western Australia, were identified. Characterisation of putative functions suggests that the bacterial community is capable of mediating the biogeochemical cycle of gold. Based the structural and chemical analysis of gold particles and secondary gold concentrations within soil, the turnover rate (or *in-situ* kinetics) of gold by biogeochemical cycling at Donnybrook was estimated to be 1.40×10^{-9} M $year^{-1}$. The

experiments involving the enrichments demonstrated that the community was sensitive to low concentrations of soluble gold. While the representative community was retained, metal-resistant bacteria were selected with higher concentrations of soluble gold. Therefore, the study suggests that gold concentrations comparable to that which was calculated in the turnover rate would provide enough metal stress allowing the biofilm to become gold-resistant over time yet retain bacterial diversity. From an environmental perspective, the availability of water is important for the continuum of gold biogeochemical cycling since microbial growth and biofilm development are dependent upon it. Additionally, the overall dissolution of gold particles and a biofilm's increased resistance to the toxicity of soluble gold highlights how the biogeochemical cycling of gold can select for metal-resistant bacteria and promote gold particle transformation in the natural environment. In conclusion, biogeochemical gold cycling directly influences bacterial communities on gold particles, thereby contributing to a continuum of particle transformation.

Acknowledgements

Funding for this research was made possible by the Australian Research Council Future Fellowship (ARC-FT100150200) awarded to F. Reith. Electron microscopy and microanalysis was performed at Adelaide Microscopy, an Australian Microscopy and Microanalysis Research Facility. The authors would like to thank Dr. M.A.D. Rea, Dr. A. Basak, Dr. B. Wade, Dr. J. Zhao, K. Neubauer and T. Reith for their technical support. Special thanks to C. Daw and T. Fowler for their excellent support in the field and with sample processing.

Conflict of Interest

The authors declare no conflict of interest.

References

Abaye D, Lawlor K, Hirsch P et al. Changes in the microbial community of an arable soil caused by long-term metal contamination. *Eur J Soil Sci* 2005;**56**: 93-102.

Anderson M, Gorley R. PERMANOVA? for PRIMER: 450 guide to software and statistical methods. PRIMER-E, Plymouth 2007.

Andrews S. FastQC: a quality control tool for high throughput sequence data. 2010.

Backhouse J, Wilson A. New records of Permian and Cretaceous sediments from the southwestern part of the Yilgarn Block. Western Australia Geological Survey Professional Papers Report 1989;**25**.

Baker W. The role of humic acid in the transport of gold. *Geochim Cosmochim Acta* 1978;**42**: 645-9.

Bååth E. Effects of heavy metals in soil on microbial processes and populations (a review). *Water Air and Soil Pollut* 1989;**47**: 335-79.

Beech IB, Sunner J. Biocorrosion: towards understanding interactions between biofilms and metals. *Curr Opin Biotechnol* 2004;**15**: 181-6.

Benedetti M, Boulëgue J. Mechanism of gold transfer and deposition in a supergene environment. *Geochim Cosmochim Acta* 1991;**55**: 1539-47.

Bennett DL, Richard J. Environmental impacts and production effects of subsurface drainage at an intensive apple orchard near Donnybrook, WA-Resource Management Technical Report 228. Department of Agriculture, Western Australia 2002.

Besemer K, Peter H, Logue JB et al. Unraveling assembly of stream biofilm communities. *ISME J* 2012;**6**: 1459.

Bezawada J, Hoang N, More T *et al*. Production of extracellular polymeric substances (EPS) by *Serratia* sp. 1 using wastewater sludge as raw material and flocculation activity of the EPS produced. *J Environ Manag* 2013;**128**: 83-91.

Bissett A, Fitzgerald A, Meintjes T *et al.* Introducing BASE: the Biomes of Australian Soil Environments soil microbial diversity database. *GigaScience* 2016;**5**: 21.

Bowles J. Mechanical and chemical modification of alluvial gold. *Australasian Institute of Mining and Metallurgy Proceedings* volume 293, 1988, 9-11

Boyle RW. *The geochemistry of silver and its deposits: with notes on geochemical prospecting for the element*: Department of Energy, Mines, and Resources, 1968.

Bray JR, Curtis JT. An ordination of the upland forest communities of southern Wisconsin. Ecol Monogr 1957;**27**: 325-49.

Bütof L, Wiesemann N, Herzberg M *et al.* Synergistic gold–copper detoxification at the core of gold biomineralisation in *Cupriavidus metallidurans*. *Metallomics* 2018; **10 (2)**, 278–286.

Cohen D, Waite T. Interaction of aqueous Au species with goethite, smectite and kaolinite. *Geochem-Explor Env A* 2004;**4:** 279-87.

Clarke KR, Gorley R, Somerfield P et al. Change in marine communities: an approach to statistical analysis and interpretation: Primer-E Ltd, 2014.

Ding Z, Bourven I, Guibaud G *et al.* Role of extracellular polymeric substances (EPS) production in bioaggregation: application to wastewater treatment. *Appl Microbiol Biotechnol* 2015;**99**: 9883-905.

Fairbrother L, Etschmann B, Brugger J *et al.* Biomineralization of gold in biofilms of *Cupriavidus metallidurans*. *Environ Sci Technol* 2013;**47**: 2628-35.

Fairbrother L, Shapter J, Brugger J *et al.* Effect of the cyanide-producing bacterium *Chromobacterium violaceum* on ultraflat Au surfaces. *Chem Geol* 2009;**265**: 313-20.

Falconer D, Craw D. Supergene gold mobility: a textural and geochemical study from gold placers in southern New Zealand. Economic Geology Special Publication 2009;14: 77-93.

Freeman M, Donaldson M. *Major Mineral Deposits of Southwestern Western Australia: A Field Guide*: Geological Survey of Western Australia, 2004.

Gatellier J-P, Disnar J-R. Organic matter and gold-ore association in a hydrothermal deposit, France. *Appl Geochem* 1989;**4**: 143-9.

Geological Survey of Western Australia Assessment of Mineral and Hydrocarbon Resources in the South-West Forest Region of Western Australia. 1998.

Gray D. *The aqueous chemistry of gold in the weathering environment*: Cooperative Research Centre for Landscape Evolution and Mineral Exploration, 1998.

Harrison JJ, Ceri H, Turner RJ. Multimetal resistance and tolerance in microbial biofilms. *Nat Rev Microbiol* 2007;**5**: 928-38.

Hough RM, Butt CR, Fischer-Bühner Jr. The crystallography, metallography and composition of gold. *Elements* 2009;**5**: 297-302.

Johnston CW, Wyatt MA, Li X *et al.* Gold biomineralization by a metallophore from a gold-associated microbe. *Nat Chem Biol* 2013;**9**: 241-3.

Korobushkina E, Karavaiko G, Korobushkin I. Biochemistry of gold. Ecological Bulletins 1983: 325-33.

Korobushkina E, Mineev G, Praded G. Mechanism of microbiological dissolution of gold. *Mikrobiologiia* 1976;**45**: 535-8.

Karthikeyan S, Beveridge T. *Pseudomonas aeruginosa* biofilms react with and precipitate toxic soluble gold. *Environ Microbiol* 2002;**4**: 667-75.

Kenney JP, Song Z, Bunker BA et al. An experimental study of Au removal from solution by non-metabolizing bacterial cells and their exudates. *Geochim Cosmochim Acta* 2012;**87**: 51-60.

Kızılkaya R, Aşkın T, Bayraklı B et al. Microbiological characteristics of soils contaminated with heavy metals. *Eur J Soil Biol* 2004;**40**: 95-102.

Lengke M, Southam G. Bioaccumulation of gold by sulfate-reducing bacteria cultured in the presence of gold (I)-thiosulfate complex. *Geochim Cosmochim Acta* 2006;**70**: 3646-61.

Lengke MF, Ravel B, Fleet ME *et al.* Mechanisms of gold bioaccumulation by filamentous cyanobacteria from gold (III)− chloride complex. *Environ Sci Technol* 2006;**40**: 6304-9.

Lengke MF, Southam G. The deposition of elemental gold from gold (I)-thiosulfate complexes mediated by sulfate-reducing bacterial conditions. *Econ Geol* 2007;**102**: 109-26.

Levipan HA, Avendano-Herrera R. Different phenotypes of mature biofilm in Flavobacterium psychrophilum share a potential for virulence that differs from planktonic state. *Soil Biol Biochem* 2017;**7**: 76.

Macdonald CA, Clark IM, Zhao F-J et al. Long-term impacts of zinc and copper enriched sewage sludge additions on bacterial, archaeal and fungal communities in arable and grassland soils. *Soil Biol Biochem* 2011;**43**: 932-41.

Magoč T, Salzberg SL. FLASH: fast length adjustment of short reads to improve genome assemblies. *Bioinformatics* 2011;**27**: 2957-63.

Mann A. Mobility of gold and silver in lateritic weathering profiles; some observations from Western Australia. *Econ Geol* 1984;**79**: 38-49.

McHugh J. Concentration of gold in natural waters. *J Geochem Explor* 1988;**30**: 85-94.

Mergeay M, Nies D, Schlegel H et al. Alcaligenes eutrophus CH34 is a facultative chemolithotroph with plasmid-bound resistance to heavy metals. *J Bacteriol* 1985;**162**: 328-34.

Mossman DJ, Dyer BD. The geochemistry of Witwatersrand-type gold deposits and the possible influence of ancient prokaryotic communities on gold dissolution and precipitation. *Precambrian Res* 1985;**30**: 303-19.

Rea MAD, Wulser P-A, Brugger J *et al*. Effect of physical and biogeochemical factors on placer gold transformation in mountainous landscapes of Switzerland. *Gondwana Res 2019;* **66**: 77-92.

Rea MA, Standish CD, Shuster J *et al.* Progressive biogeochemical transformation of placer gold particles drives compositional changes in associated biofilm communities. *FEMS Microbiol Ecol* 2018;**94**: fiy080.

Rea MA, Zammit CM, Reith F. Bacterial biofilms on gold grains-implications for geomicrobial transformations of gold. *FEMS Microbiol Ecol* 2016;**92**: fiw082.

Reith F, Brugger J, Zammit CM *et al.* Influence of geogenic factors on microbial communities in metallogenic Australian soils. *ISME J* 2012;**6**: 2017.

Reith F, Brugger J, Zammit CM *et al.* Geobiological cycling of gold: from fundamental process understanding to exploration solutions. *Minerals* 2013;**3**: 367-94.

Reith F, Cornelis G. Effect of soil properties on gold-and platinum nanoparticle mobility. *Chem Geol* 2017;**466**: 446-53.

Reith F, Etschmann B, Grosse C *et al.* Mechanisms of gold biomineralization in the bacterium *Cupriavidus metallidurans*. *Proc Natl Acad Sci USA* 2009;**106**: 17757-62.

Reith F, Fairbrother L, Nolze G *et al.* Nanoparticle factories: Biofilms hold the key to gold dispersion and nugget formation. *Geology* 2010;**38**: 843-6.

Reith F, Lengke MF, Falconer D *et al.* The geomicrobiology of gold. *ISME J* 2007;**1**: 567-84.

Reith F, McPhail D. Mobility and microbially mediated mobilization of gold and arsenic in soils from two gold mines in semi-arid and tropical Australia. *Geochim Cosmochim Acta* 2007;**71**: 1183-96.

Reith F, McPhail DC. Effect of resident microbiota on the solubilization of gold in soil from the Tomakin Park Gold Mine, New South Wales, Australia. *Geochim Cosmochim Acta* 2006;**70**: 1421-38.

Reith F, McPhail D, Christy A. Bacillus cereus, gold and associated elements in soil and other regolith samples from Tomakin Park Gold Mine in southeastern New South Wales, Australia. *J Geochem Explor* 2005;**85**: 81-98.

Reith F, Rea MAD, Sawley P *et al.* Biogeochemical cycling of gold: Transforming gold particles from arctic Finland. *Chem Geol* 2018;**483**: 511-29.

Reith F, Rogers S. Assessment of bacterial communities in auriferous and non-auriferous soils using genetic and functional fingerprinting. *Geomicrobiology J* 2008;**25**: 203-15

Reith F, Rogers SL, McPhail D *et al.* Biomineralization of gold: biofilms on bacterioform gold. *Science* 2006;**313**: 233-6.

Reith F, Stewart L, Wakelin SA. Supergene gold transformation: Secondary and nano-particulate gold from southern New Zealand. *Chem Geol* 2012;**320**: 32-45.

Reith F, Zammit CM, Pohrib R *et al.* Geogenic factors as drivers of microbial community diversity in soils overlying polymetallic deposits. *Appl Environ Microbiol* 2015: AEM. 01856-15.

Sanyal SK, Shuster J & Reith F (2019) Cycling of biogenic elements drives biogeochemical gold cycling. *Earth-Sci Rev* 190: 131-147.

Settimio L, McLaughlin MJ, Kirby JK *et al.* Fate and lability of silver in soils: Effect of ageing. *Environ Pollut* 2014;**191**: 151-7.

Schröfel A, Kratošová G, Bohunická M *et al*. Biosynthesis of gold nanoparticles using diatoms—silica-gold and EPS-gold bionanocomposite formation. *J Nanoparticle Res* 2011*;* **13**: 3207-3216.

Shuster J, Bolin T, MacLean LC *et al.* The effect of iron-oxidising bacteria on the stability of gold (I) thiosulphate complex. *Chem Geol* 2014;**376**: 52-60.

Shuster J, Johnston CW, Magarvey NA *et al.* Structural and chemical characterization of placer gold grains: implications for bacterial contributions to grain formation. *Geomicrobiol J* 2015;**32**: 158-69.

Shuster J, Marsden S, Maclean LC *et al.* The immobilization of gold from gold (III) chloride by a halophilic sulphate-reducing bacterial consortium. *Geological Society, London, Special Publications* 2015;**393**: 249-63.

Shuster J & Reith F (2018) Reflecting on Gold Geomicrobiology Research: Thoughts and Considerations for Future Endeavors. *Minerals* **8**: 401.

Shuster J, Reith F, Cornelis G *et al*. Secondary gold structures: Relics of past biogeochemical transformations and implications for colloidal gold dispersion in subtropical environments. *Chem Geol* 2017;**450**: 154-64.

Shuster J, Reith F, Izawa MR *et al.* Biogeochemical cycling of silver in acidic, weathering environments. *Minerals* 2017;**7**: 218.

Smith AD, Hunt RJ. Solubilisation of gold by *Chromobacterium violaceum*. *J Chem Technol Biotechnol* 1985;**35**: 110-6.

Song JY, Jang H-K, Kim BS. Biological synthesis of gold nanoparticles using Magnolia kobus and Diopyros kaki leaf extracts. *Process Biochem* 2009;**44**: 1133-8.

Southam G, Beveridge TJ. The in vitro formation of placer gold by bacteria. *Geochim Cosmochim Acta* 1994;**58**: 4527-30.

Southam G, Lengke MF, Fairbrother L *et al.* The Biogeochemistry of Gold. *Elements* 2009;**5**: 303-7.

Ta C, Reith F, Brugger Jl *et al.* Analysis of gold (I/III)-complexes by HPLC-ICP-MS demonstrates gold (III) stability in surface waters. *Environ Sci Technol* 2014;**48**: 5737-44.

Tamura K, Dudley J, Nei M *et al.* MEGA4: molecular evolutionary genetics analysis (MEGA) software version 4.0. *Mol Biol Evol* 2007;**24**: 1596-9.

Thomas L. Regolith-Landforms and plant biogeochemical expression of buried mineralisation targets in the Northern Middleback Ranges,(“Iron Knob South”) South Australia, 2011.

Townley BK, Hérail G, Maksaev V et al. Gold grain morphology and composition as an exploration tool: application to gold exploration in covered areas. *Geochem-Explor Env A* 2003;**3**: 29-38

Wakelin S, Anand RR, Macfarlane C et al. Assessing microbiological surface expression over an overburden-covered VMS deposit. *J Geochem Explor* 2012a;**112**: 262-71.

Wakelin S, Anand RR, Reith F et al. Bacterial communities associated with a mineral weathering profile at a sulphidic mine tailings dump in arid Western Australia. *FEMS Microbiol Ecol* 2012b;**79**: 298-311.

Wang X, Xie X, Ye S. Concepts for geochemical gold exploration based on the abundance and distribution of ultrafine gold. *J Geochem Explor* 1995;**55**: 93-101.

Webster J, Mann A. The influence of climate, geomorphology and primary geology on the supergene migration of gold and silver. *J Geochem Explor* 1984;**22**: 21-42.

Wiesemann N, Bütof L, Herzberg M et al. Synergistic toxicity of copper and gold compounds in *Cupriavidus metallidurans*. *Appl Environ Microbiol* 2017;**83**: e01679-17.

Wollast R, Mackenzie F. Global biogeochemical cycles and climate. *Climate and Geo-sciences*: Springer, 1989, 453-73.

Zammit CM, Weiland F, Brugger J *et al.* Proteomic responses to gold (iii)-toxicity in the bacterium *Cupriavidus metallidurans* CH34. *Metallomics* 2016;**8**: 1204-1216.

Zhu LD, Zhao TS, Xu JB et al. Preparation and characterization of carbon-supported sub-monolayer palladium decorated gold nanoparticles for the electro-oxidation of ethanol in alkaline media. *J Power Sources* 2009;**187**: 80-4.

Figure 1

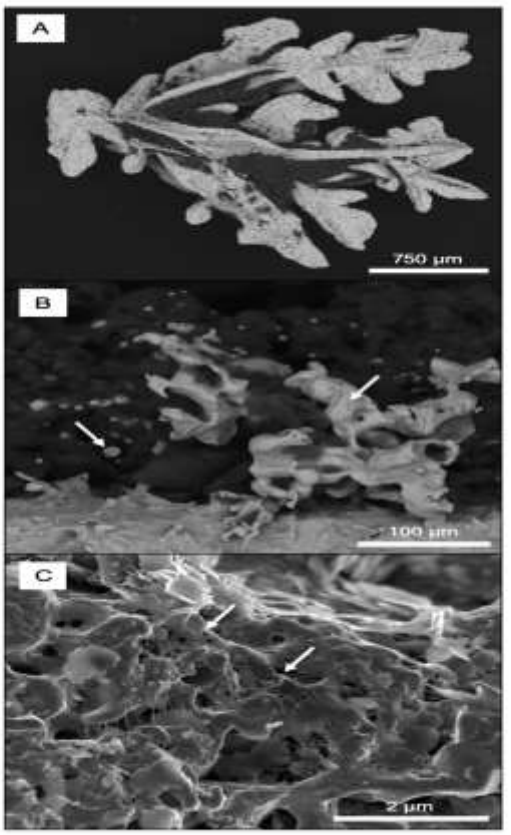

Figure 1. Backscatter electron (BSE) SEM micrograph of a representative gold particle from Donnybrook, Western Australia (A). The surface of gold particles contained gold dissolution features (right arrow, B) and secondary gold nanoparticles (left arrow, B). Some gold nanoparticles occurred as pseudo-spheres and euhedral crystals that were partially embedded within the clay minerals (B). A high-magnification secondary electron (SE) SEM micrograph demonstrating the presence of exopolymeric substances (arrows, C).

Figure 2

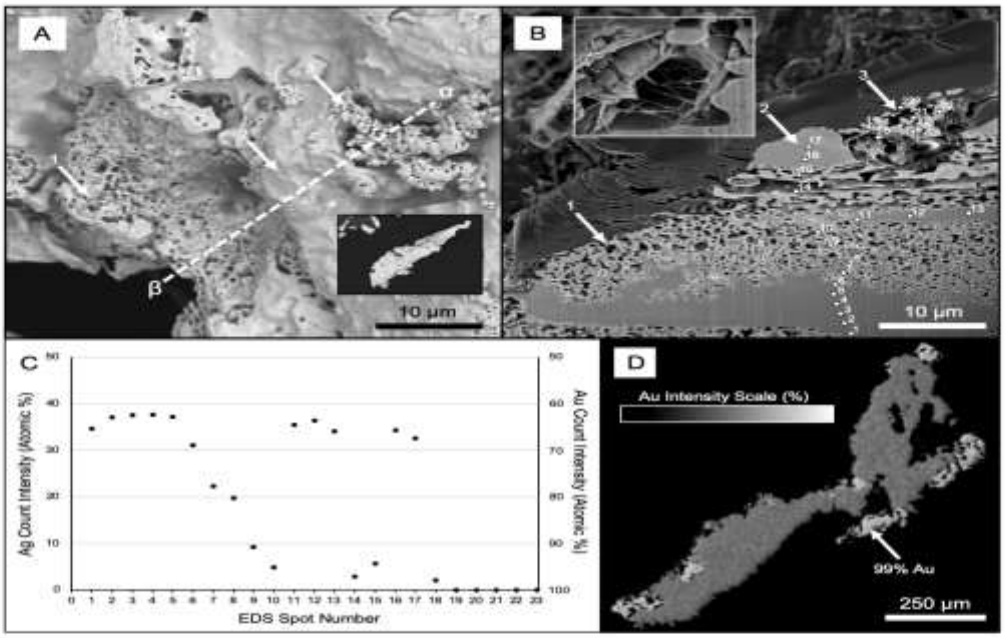

Figure 2. A high-magnification BSE SEM micrograph of gold dissolution features (arrow one, A) along with an aggregation of secondary Au nanoparticles (arrow three, A) from a particle (inset, A). A SE SEM micrograph of a FIB-milled cross-section through the gold dissolution feature. Note that the FIB-milled cross-section corresponds to the α-β line in Figure 2A and the number arrows point at corresponding features: (1) dissolution feature, (2) a 'ridge', (3) aggregated secondary gold nanoparticles. The aggregated secondary gold nanoparticles occurred directly above the gold dissolution feature (arrow 3, B). These dissolution features appeared as network of cavities at the surface of the gold particle (B). Some pores spaces contained EPS (inset, B). A series of spot analysis by Energy Dispersive Spectroscopy corresponding to the locations illustrated in Figure 2B (C). A representative EMPA gold-intensity maps of a gold particle. The outer edge of the particle contained an enrichment of secondary pure (≥99.0%) gold (D).

Figure 3

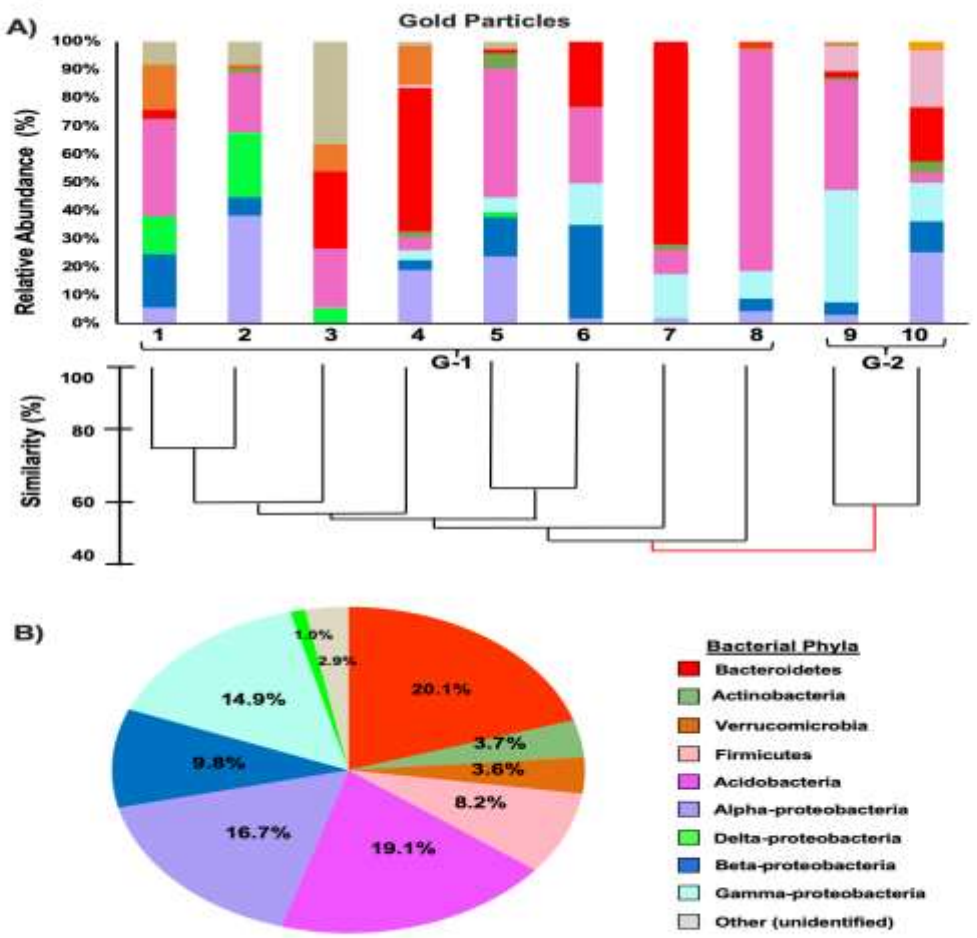

Figure 3. The taxonomic distribution and relative abundance of bacterial communities on ten individual particles and the cluster analysis demonstrating the similarity between the communities from each particle (A). A pie chart showing the average taxonomic distribution from bacterial communities on all 10 particles (B); note that taxonomic classes are shown for the Proteobacteria.

Figure 4

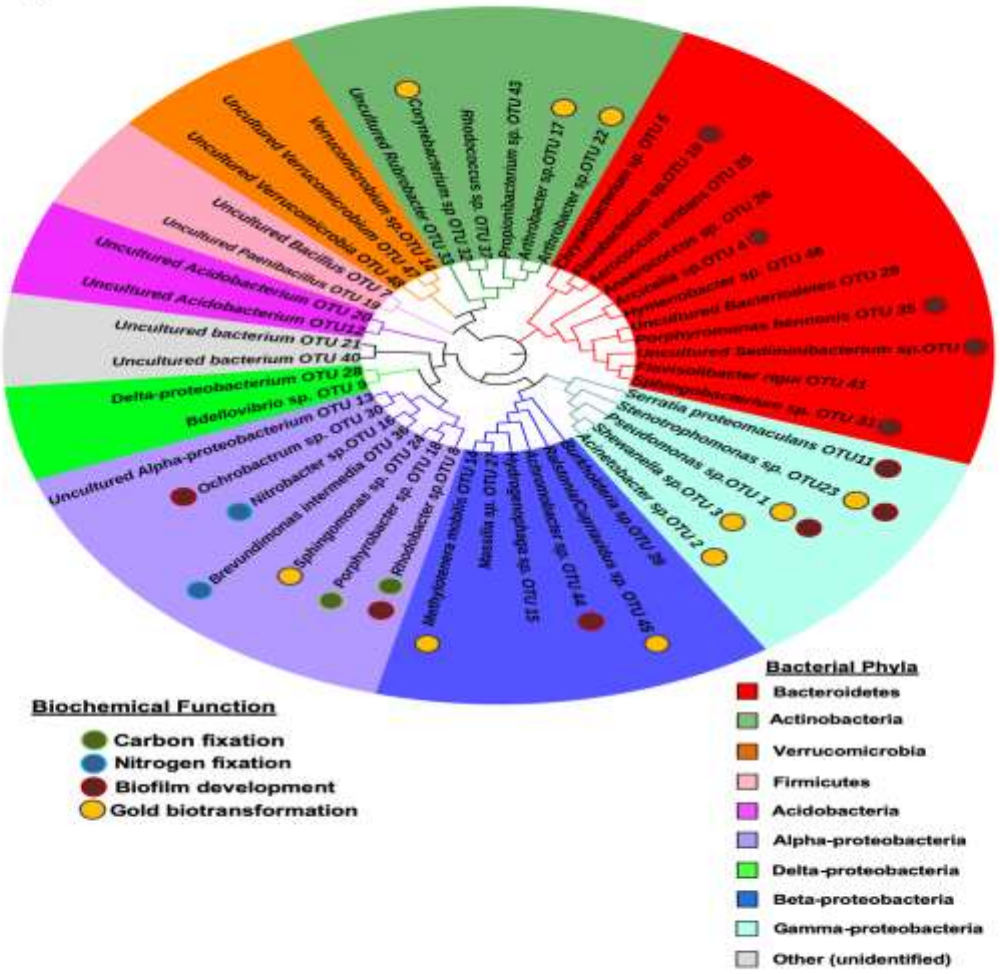

Figure 4. A neighbor-joining circular cladogram of bacterial OTUs demonstrating the diversity of bacterial species. Colored circles indicate putative biochemical functions necessary.

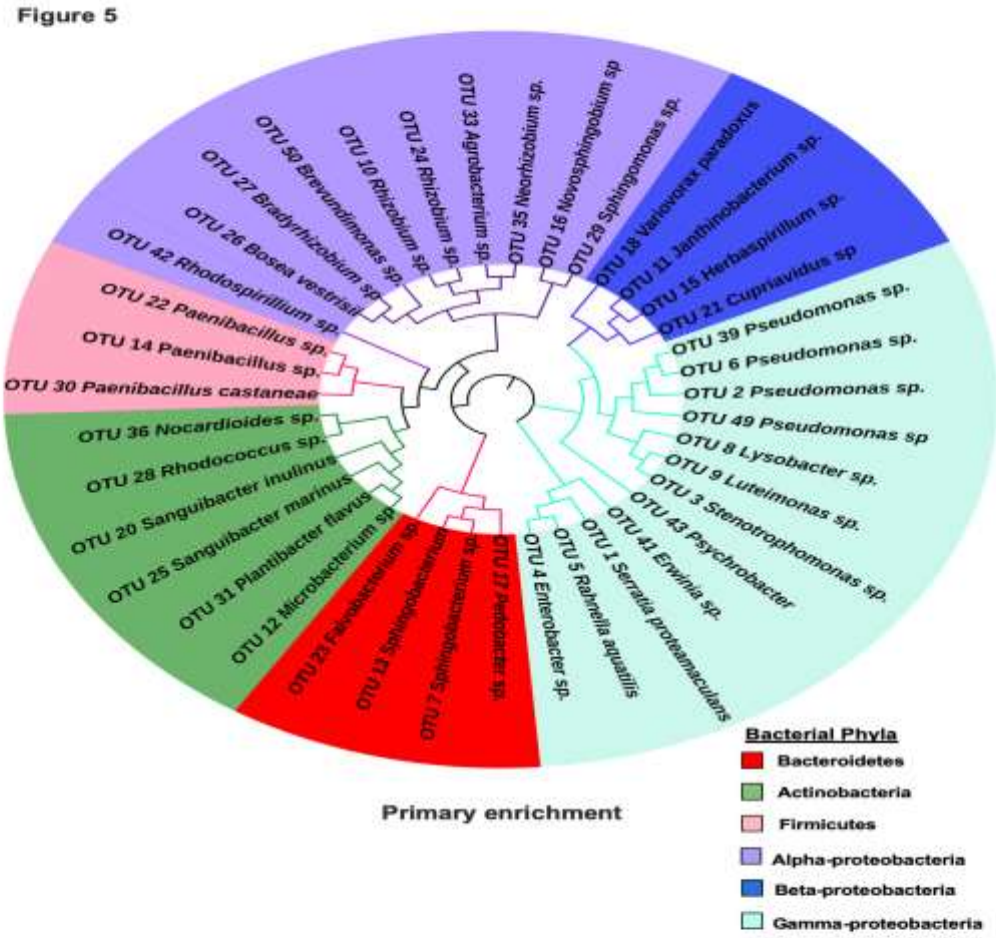

Figure 5. Circular cladogram of the bacterial OTUs detected in the primary enrichment culture.

Figure 6

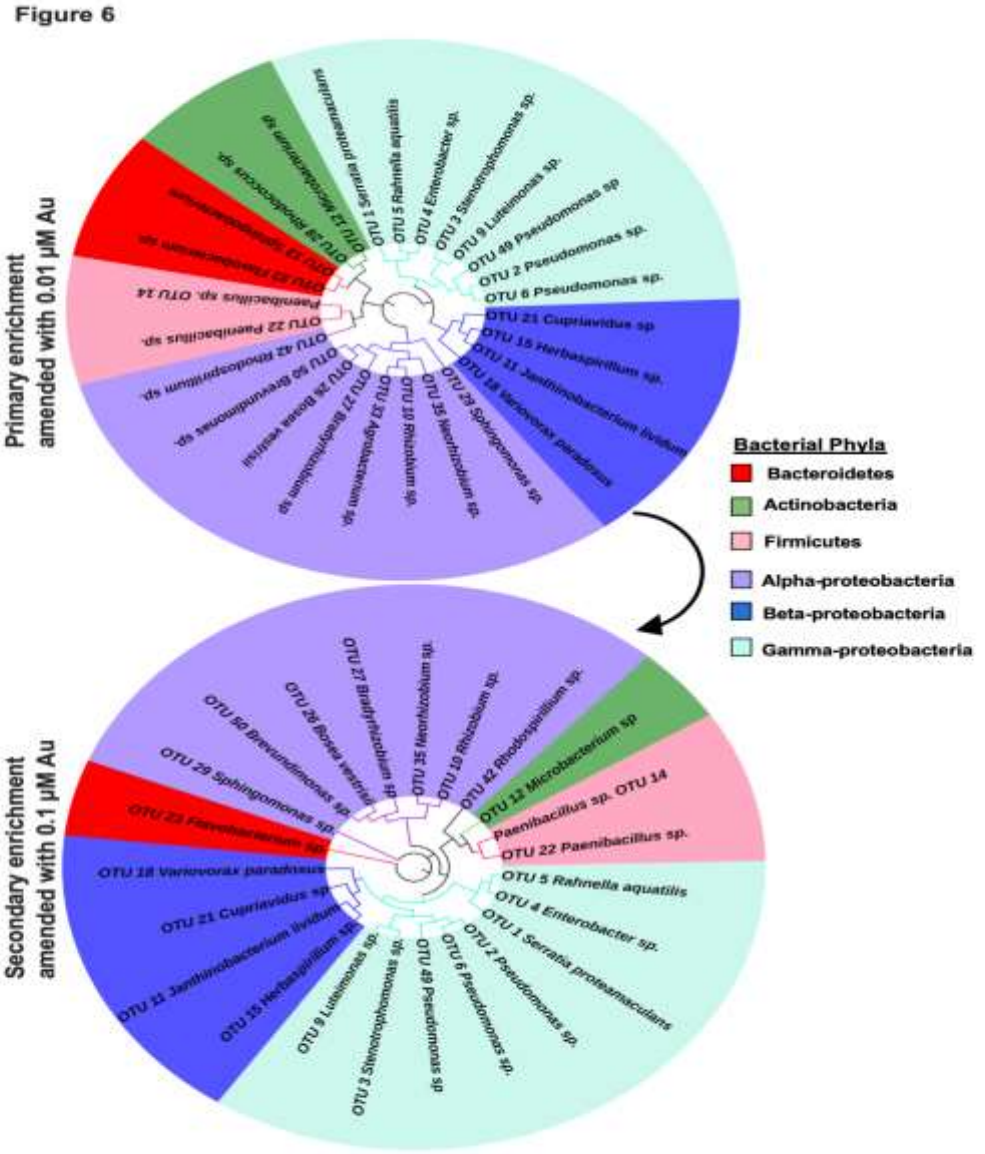

Figure 6. Circular cladograms of the bacterial OTUs from the primary enrichment amended with 0.01 µM Au and the secondary enrichment amended with 0.1 µM Au (i.e., the low gold concentration group). Note that these concentrations represent elevated gold concentrations in natural environments.

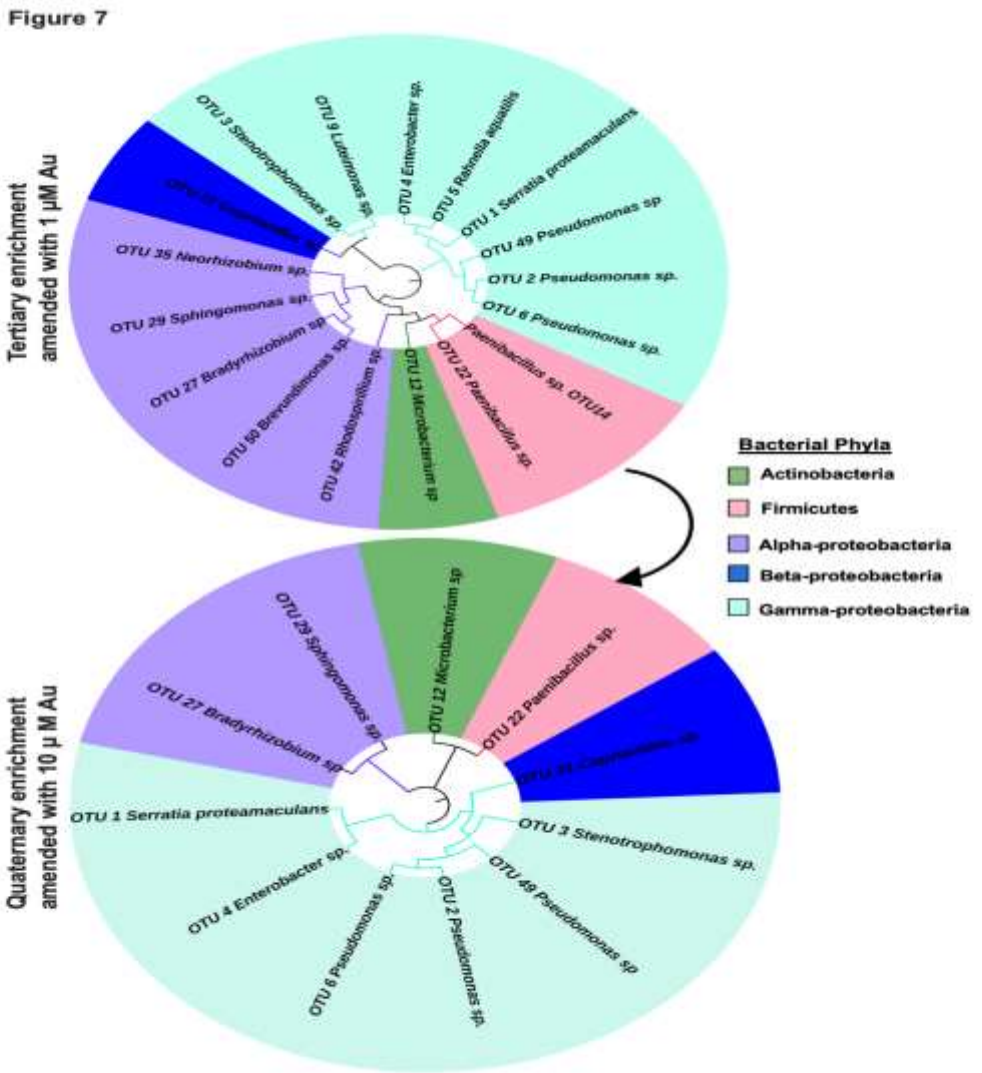

Figure 7. Circular cladograms of the bacterial OTUs from the tertiary enrichment amended with 1 µM Au and the quaternary enrichment amended with 10 µM Au (i.e., the high gold concentration group). Note that these concentrations represent highly anomalous gold concentrations in natural environments.

Figure 8

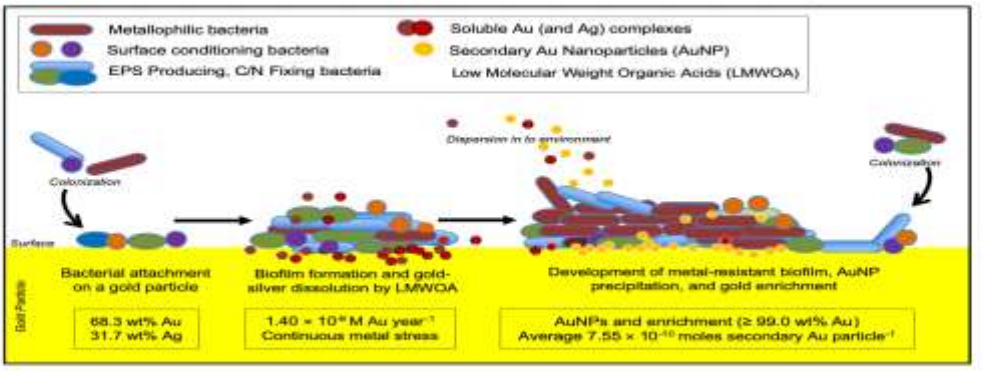

Figure 8. A schematic diagram representing the effect of gold biogeochemical cycling on bacteria and the development of a metal resistant biofilm contributing to particle transformation and the continuum of gold biogeochemical cycling.

Table 1. Calculations for estimating the rate of (bio)geochemical gold cycling within mullock heaps at Donnybrook, Australia, using EMP data of gold particles and ICP-MS data of soil.

Particle	Au (wt. %) [a]	Ag (wt.%) [b]	Volume of Particle (cm^3) [c]	Volume of Particle 'Slice' (cm^3) [d]	Volume of Secondary Au per Slice (cm^3) [e]	Multiplication Factor [f]	Total Volume of Secondary Au (cm^3) [g]	Mass of Secondary Au (g) [h]	Moles of Secondary Au [i]
1	70	30	2.75×10^{-5}	6.65×10^{-10}	4.43×10^{-11}	4.14×10^{4}	1.83×10^{-6}	9.50×10^{-8}	4.82×10^{-10}
2	65	35	2.85×10^{-5}	1.15×10^{-10}	8.83×10^{-12}	2.48×10^{5}	2.18×10^{-6}	1.13×10^{-7}	5.74×10^{-10}
3	68	32	2.79×10^{-5}	3.97×10^{-10}	1.61×10^{-6}	7.02×10^{4}	3.01×10^{-6}	1.56×10^{-7}	7.91×10^{-10}
4	70	30	2.75×10^{-5}	1.65×10^{-09}	6.42×10^{-7}	1.67×10^{4}	1.18×10^{-6}	6.11×10^{-8}	3.10×10^{-10}
5	72	28	2.72×10^{-5}	5.31×10^{-10}	3.69×10^{-6}	5.12×10^{4}	6.70×10^{-6}	3.47×10^{-7}	1.76×10^{-9}
6	65	35	2.85×10^{-5}	2.41×10^{-10}	1.22×10^{-6}	1.18×10^{5}	1.22×10^{-6}	1.21×10^{-7}	6.12×10^{-10}
Average								7.55×10^{-10}	
60 particles [j]								4.53×10^{-8}	
Moles of secondary gold in 100 kg soil (extrapolated) [k]					1.17×10^{-4}				
Total Moles of Secondary Gold in 100 kg soil [l]					1.17×10^{-4}				
Rate of (Bio)geochemical Gold Cycling (M $year^{-1}$) [m]					1.40×10^{-9}				

[a] Weight percent of gold determined by EMP analysis.

[b] Weight percent of silver determined by EMP analysis.

[c] Particle volume = ((a × average mass of a particle) ÷ gold density) + ((b × average mass of a particle) ÷ silver density)

[d] Volume of particle slice = Particle slice area × average sampling depth

[e] Volume of secondary gold per particle 'slice' = Secondary gold area × average sampling depth.

[f] Multiplication factor = c ÷ d

[g] Total volume of secondary gold = e × f

[h] Mass of secondary gold = g ÷ density of gold

[i] Moles of secondary gold = h ÷ molar mass of gold

[j] Moles of secondary gold for 60 particles = average moles of secondary gold × 60

[k] Moles of secondary gold in 100 kg soil = (Gold concentration determined by ICP-MS ÷ molar mass of gold) × 100 kg

[l] Total moles of secondary gold in 100 kg soil = j + k

[m] Rate of gold (bio)geochemical cycling = l ÷ minimum number of year gold occurred in mullock heaps ÷ average annual rainfall

Supporting Information:

Supplemental Methods: PCR and Sequencing

Table S2. List of primers used in the study

Table S2. Elemental composition of soil samples from Donnybrook, Western Australia